I.

MTL MICROSYSTEMS TECHNOLOGY LABORATORIES

mtl.mit.edu

MMS (Möbius Metamaterial Strips): Opportunity, Emerging Trends, Challenges, and Future Directions

Authors:

Ajay K. Poddar (1) , Ulrich L. Rohde (1, 2,),

Author affiliations:

(1) Synergy Microwave, NJ, USA

(2) Massachusetts Institute of Technology, MIT, Microsystems Technology Laboratories, USA

Based on [73, 74]

Introduction

MMS (Metamaterial Möbius-Strip) is an artificial composite structure, exhibits negative index ($n = -\sqrt{\epsilon\mu}$; $\varepsilon < 0$, $\mu < 0$, where n is refractive index, ε is electric permittivity of medium, and μ is magnetic permeability of medium) characteristics, and have emerged as a cutting-edge science, relating physics, chemistry, biology, optics, acoustics, electronics, and material science. For most of the naturally existing materials, the magnetic permeability (μ) is close to 1; hence magnetic susceptibility of natural materials is small as compared to the electric/dielectric susceptibility. This phenomenon limits the interaction of atoms to the electric component of the electromagnetic (EM) wave and leaving the magnetic component mostly unexploited. And, magnetism is primarily weak at optical frequencies, because the relaxation times of paramagnetic and ferromagnetic processes are considerably longer than the optical period, and thus the electron movement in atoms is the only mechanism for the magnetic response. That's why, the magnetic field component usually is not involved in light-matter interactions. The reason of weak magnetism is mainly due to limitations of the material properties imposed by their chemical composition and constituent components (atoms and molecules). On the contrary, MMS (Metamaterial Möbius-Strip) resonant nanostructures in principle, can exhibit a broad range of values of magnetic permeability[1-75]. A number of stimulating phenomena and applications associated with MMS structures are discussed in Part-1 (MWJ May 2016) and Part-2 (MWJ June 2016) issue, this issue addresses the prospect, challenges and future directions of MMS inspired components for various applications including Gravitational Casimir effect.

Recent research activities[69-75] in the field of Metamaterial (negative index material) has not only established interesting physical phenomena but also lead to opportunity for utilizing negative index components and devices for next generation energy-efficient electronic circuits and systems. Figure (1) shows the typical characteristics of the medium that explains the properties of natural and artificially engineered composite material[1]. Unlike conventional materials that interact with EM (electromagnetic) wave based on their chemical composition, the properties of Metamaterial are derived from their topology and geometric structure.

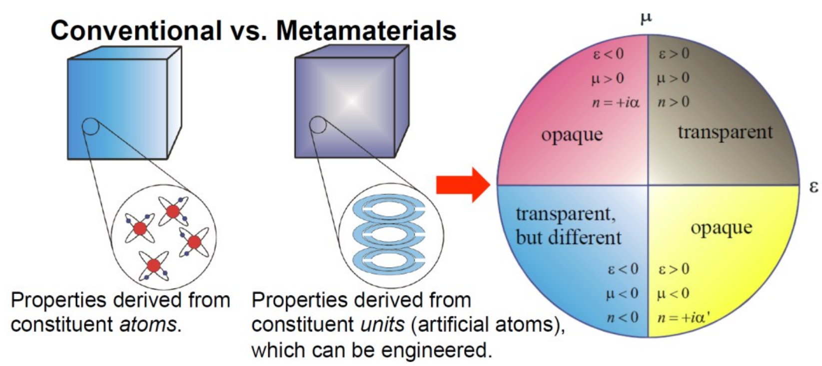

Fig.1 shows the characteristics of conventional and Metamaterial

As shown in Figure (1), the typical Metamaterial consists of periodically or arbitrarily disseminated structured cells, whose dimension and spacing are much smaller than the wavelength of incident electromagnetic waves (EM)[1-3]. As a consequence, the microscopic detail of each unit cell structure cannot be sensed by EM waves. What is important to understand here is the average result of the collective response of the entire assemblage comprises of inhomogeneous matter. In other words, such a collection of inhomogeneous matter can be characterized by an equivalent homogenous material with effective constitutive relative permittivity ($\varepsilon_{r,eff}$) and permeability ($\mu_{r.efff}$) at the macroscopic level. The key aspect of MMS inspired structure is that effective permittivity ($\varepsilon_{r,eff}$) and permeability ($\mu_{r.efff}$) can be controlled and tuned by suitably designed disseminated element for broadband operation.

In classical EM (electromagnetics), the characteristics of matter illustrated in Figure (1) can be described by the Drude–Lorentz model[6] as

$$\varepsilon_r(\omega) = \left[1 - \left(\frac{\omega_{p,e}^2}{\omega^2 - \omega_{0,e}^2 + i\omega\gamma_e}\right)\right] \tag{1}$$

$$\mu_r(\omega) = \left[1 - \left(\frac{\omega_{p,m}^2}{\omega^2 - \omega_{0,m}^2 + i\omega\gamma_m}\right)\right] \tag{2}$$

where ω_p is the plasma frequency, ω_0 is the resonant frequency, subscripts '*e*' and '*m*' represent electric and magnetic response, and γ is the damping factor associated to material losses.

Figure (2) shows the typical Metamaterial[4-5] structure, realized by combination of SRR (split ring resonators) and thin metallic wires; the effective relative permittivity ($\varepsilon_{r,eff}$) and effective relative permeability ($\mu_{r.efff}$) obeys the Drude–Lorentz[6-9] model as

$$\varepsilon_{r,eff}(\omega) = \left[1 - \left(\frac{\omega_{p,eff}^2}{\omega(\omega + i\omega\gamma_{eff})}\right)\right] \tag{3a}$$

$$\omega_{p,eff}^2 = \frac{e^2}{\varepsilon_0}\left(\frac{n_{e,eff}}{m_{e,eff}}\right) = \frac{2\pi c^{\ 2}}{d^2\left(\ln\frac{d}{r}\right)} \tag{3b}$$

$$\gamma_{eff} = \varepsilon_0\left(\frac{d^2\omega_p^2}{\pi r^2 \sigma}\right) =\cong 0.1\omega_{p,eff} \tag{3c}$$

$$\mu_r(\omega) = 1 - \frac{F\omega^2}{\omega^2 - \omega_0^2 + i\Gamma\omega} \tag{4a}$$

$$F = \frac{\pi \times r^2}{d^2} \tag{4b}$$

$$\omega_0 = \sqrt{\frac{3sc^2}{\pi^2\ r^3}} \tag{4c}$$

$$\Gamma = \frac{2}{\mathrm{r}\sigma\mu_0} \tag{4d}$$

where σ is the conductivity of metal wire, d is the lattice constant, ω_0 represents the resonant frequency, $\omega_{p,eff}$ is the effective plasma frequency, *F* is the filling ratio of the SRR, and Γ is the damping term. From (3), assuming the metal wire conductivity $\sigma = 10^7\,\Omega^{-1}\,m^{-1}$, metal wire radius $r = 1\times10^{-6}$ meter, lattice constant $d = 3.5\times10^{-3}$ meter, the effective plasma frequency is $\omega_{p,eff} = 7.52 \times 10^{10}$ rad/sec. From (4), assuming the SRR $d = 4\times10^{-3}$ meter, $r = 1\times10^{-3}$ meter, and $s = 1\times10^{-4}$ meter; the resonant frequency $f_0 = 8.324\ GHz$, which corresponds to a free space wavelength of 3.6×10^{-2} meter which is about 10 times larger than that of lattice constant *d*.

From (3) and (4), the effective permittivity ($\varepsilon_{r,eff}$) of metallic wire and effective permeability ($\mu_{r.efff}$) of SRR exhibits the typical Drude-Lorentz characteristics[8], plotted in Figure 2 (b) and (d). Equations (3) and (4) can provide approximate analytical solution of the effective constitutive parameters (permittivity, permeability) with reasonable accuracy, valid for a simple structure shown in Figure (2). But for the complex structure, this is not true, especially for MMS (Metamaterial Möbius-Strips) inspired negative index Metasurface. The alternative approach is to retrieve the effective parameters from numerical simulations[9-12] described in detail[70]. The first step of the retrieval procedure is to calculate the transmission and reflection of the composite MMS based on numerical algorithms, such as Finite-Difference Time-Domain (FDTD) and

Finite Element Method (FEM). Some commercial software, including ADS, Ansys HFSS, CST Microwave Studio, COMSOL Multiphysics and SONNET are widely used but none of these provides error free solutions. The refractive index and impedance are related to the transmission coefficient (t) and reflection coefficient (r) by equations[9]

$$z_{eff} = \pm \left[\frac{(1+r)^2-t^2}{(1-r)^2-t^2}\right]^{1/2} \tag{5}$$

$$n_{eff} = \pm cos^{-1}\left[\frac{1}{k_0 L}\left(\frac{1-r^2+t^2}{2t}\right)\right] + \frac{2\pi m}{k_0 L}, \qquad k_0 = \frac{2\pi}{\lambda_0} \tag{6}$$

$$\varepsilon_{r,eff}(\omega) = \frac{n_{eff}(\omega)}{z_{eff}(\omega)} \tag{7}$$

$$\mu_{r,eff}(\omega) = n_{eff}(\omega) \times z_{eff}(\omega) \tag{8}$$

where k_0 is the wave vector in vacuum, L is the thickness of the Metamaterial, and m is an integer.

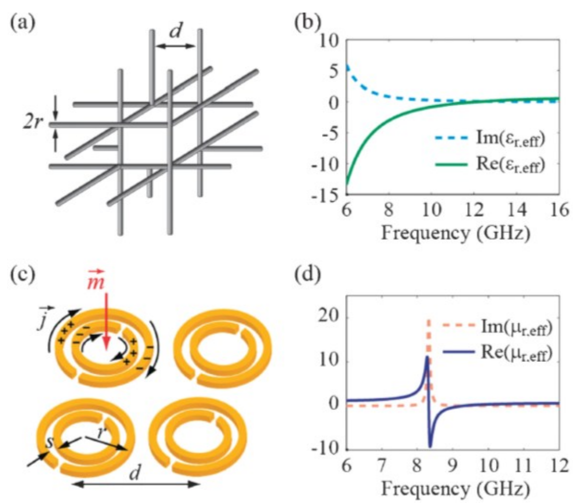

Fig. 2 A typical negative index structure for the realization of artificial electric and magnetic responses: (a) graphic of periodic wires (radius r) arranged in a simple cubic lattice (lattice constant d), (b) Effective permittivity ($\varepsilon_{r,eff}$) of wire medium, acting as dilute metals with an extremely low plasma frequency, (c) schematic of split ring resonators (SRRs), with outer radius r and separation s between the two rings; a magnetic field penetrating the SRR induces a current ($\bar{J}$), and hence a magnetic moment ($\bar{m}$),), and (d) Effective permeability ($\mu_{r.efff}$) of SRRs at resonant frequency[8].

From Equations (5) and (6), effective impedance and refractive index can be determined provided Metamaterial structures are acts like passive medium, implies that the real part of z_{eff} and the imaginary part of n_{eff} have to be positive[9]. It is to note that effective parameter retrieval process is a challenging task, especially when metamaterial structures fall into the category of anisotropic or bi-anisotropic, and EM wave is obliquely incident[12]. In addition to this, parameter retrieval becomes even more complex for nonlinear Metamaterial composite structure.

The Metamaterial structure shown in Figure (3a) is a combination of metallic wires and SRRs, these artificially engineered structures pose fabrication problems. The simplified structure reported in literature is Fishnet structure[14-16] that consists of two layers of metal meshes separated by a dielectric spacer layer (Fig. 3(b)). The paired stripes those are oriented parallel to the electric field that provides negative $\varepsilon_{r,eff}(\omega)$, while the other pairs of stripes parallel to the magnetic field support negative $\mu_{r,eff}(\omega)$. Since the spacing dielectric thickness of the fishnet structure is easy to control, significantly eases the fabrication burden as compared to the conventional approach of combing SRRs and metallic wires[8]. Moreover, EM waves are incident normal to the fishnet surface to produce the negative refractive index, this arrangement as compared to Metamaterial structure fabricated by SRRs and wires, which require oblique incidence of EM waves to excite SRRs with out-of-plane magnetic fields for strong magnetic resonances.

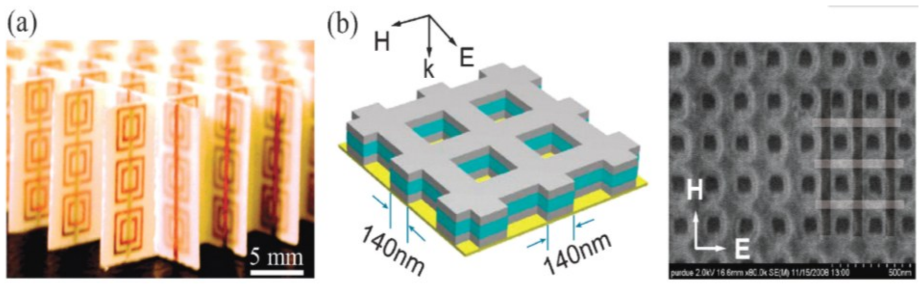

Fig. 3: A typical arrangement of artificially engineered negative index medium (Metamaterial structure): (a) works at microwave frequencies, consist of copper SRRs and wires deposited lithographically on standard circuit boards, the size of the unit cell is 5×10^{-3}meter[13], (b) Fishnet structure as NIMs in the visible region (yellow light), left panel is the schematic of the fishnet structure, in which two layers of metal meshes (gray) are separated by a dielectric layer (cyan), and the right panel is the scanning electron microscope (SEM) image of the sample fabricated by electron beam lithography (EBL)[14]

Metamaterial Opportunity and Emerging Trends

Aerospace, defense, and biomedical electronics market is often presented as the most effervescent sector of the Metamaterial based products market. The rise of drones, the need for light weight and the inevitable need for improved military communications, and biosensors are all areas where metamaterial technology can help propel things forward.

(i) Imaging

Metamaterial structures are known for magnetic imaging, microwave circuit component, antennas, and perfect lens with imaging resolution beyond the diffraction limit[1-21]. In conventional optical systems, it is not possible to determine two points separated less than $l/2n$, where n is the refractive index of the ambient medium. This fundamental limitation exists because the information of the object’s fine features and textures are carried by evanescent waves, which exponentially decay in space. All the information relevant to the sub-wavelength details of the object is lost, before reaching the imaging plane. It is interesting to note that Metamaterial slab acts as a perfect lens to recover all the lost information[20]. This extraordinary property of perfect lens arises from the fact that the initially decayed evanescent waves are now amplified through the Metamaterial slab. Meanwhile, the propagating waves are focused due to the negative refraction and reversed phase front. As a result, a Metamaterial slab incredibly brings both propagating and evanescent waves to a perfect focus (Fig. 4(a) and 4(b)), without suffering the traditional constraint imposed by the diffraction limit. This shows promising applications of metamaterial super-lenses which are lenses that are almost free of aberrations and that can focus images below the diffraction limit. The recorded image ‘‘NANO’’ (middle panel of Fig. 4(c)) reproduced the fine features from the object mask (top panel of Fig. 4(c)) in all directions with good fidelity, while the image of ‘‘NANO’’ in the control experiment without the superlens showed a much wider line width (bottom panel of Fig. 4(c)) [22]. In the seminal paper, Pendry et al. predicted the enhanced nonlinear optical properties by inserting nonlinear elements into the gap of SRRs, arising from the giant local-field amplification[5].

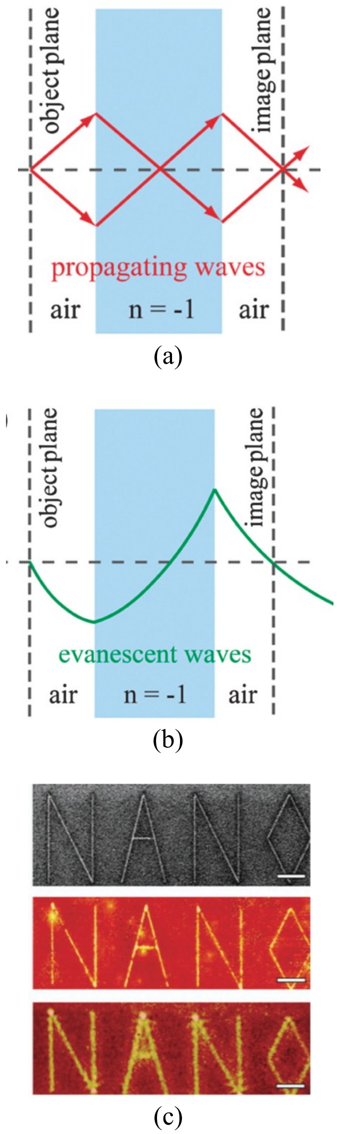

Fig. 4: Metamaterial slab shows the properties of perfect lens: (a) A typical negative index slab ($n = -\sqrt{\epsilon\mu}$=-1; ε < 0, μ < 0) can focus all the light rays from a point source, arising from the negative refraction, (b) The negative index slab can also amplify evanescent waves, leading to perfect imaging at the image plane, and (c) Experimental demonstration of an optical silver superlens

Figure (5) shows the typical measurement setup for MRI measurement at 8.5MHz for Prostate Cancer Detection. By utilizing Metamaterial inspired (μ = -1) split ring resonators loaded with capacitors and inductors enabled 20 times increase in the magnetic field. As shown in Figure (5b), with the lens (green), the lens resolves two magnetic sources that cannot be distinguished without the lens (blue) [76].

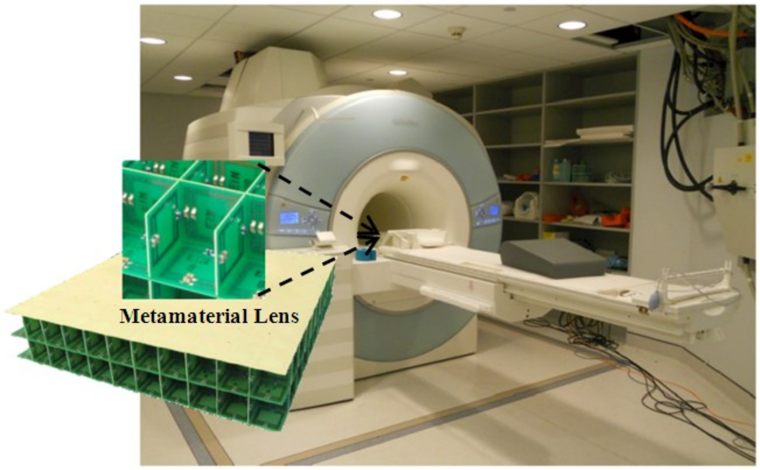

(a) Measurement setup shows the use of Metamaterial lens for imaging

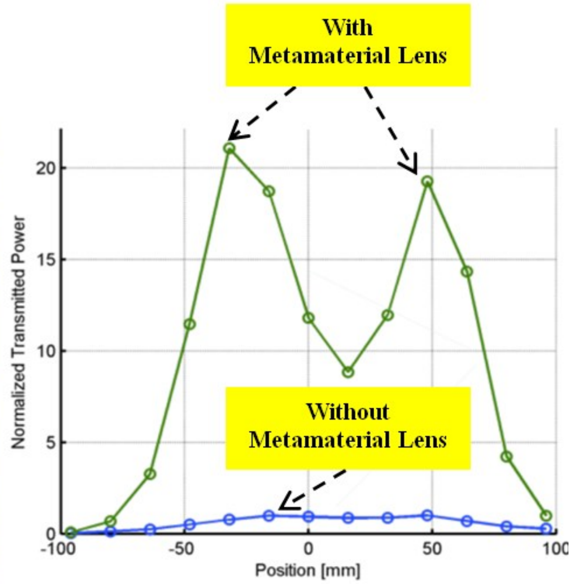

(b) Response with and without Metamaterial Lens

Fig. 5: Isotropic μ = -1 Metamaterial for MRI Enhancement at 8.5MHz for Prostate Cancer Detection: (a) MRI Measurement setup shows the use of metamaterial lens for super resolution imaging , and (b) Response with and without Metamaterial Lens[76]

(ii) Light Weight Metamaterial Conformal Antennas

Metamaterial technology is an enabler to build lighter and more compact antennas systems. Figure (6) shows the performance of the typical light weight inspired monopole antenna. As illustrated in Figure (6), the measured plots show that the Metamaterial increased the bandwidth to over an octave while preserving the radiation pattern of a simple monopole: blue line shows the simulated monopole alone, gray line exhibits measured monopole alone, red line shows simulated monopole with Metamaterial, and black line exhibits monopole with Metamaterial[77].

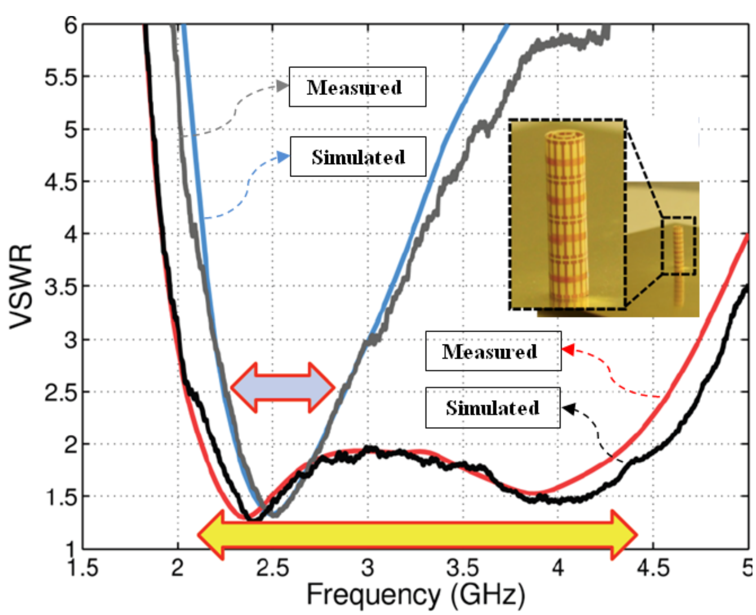

Fig.6: The measured plots show that the Metamaterial increased the bandwidth to over an octave while preserving the radiation pattern of a simple monopole[77]

(iii)Manipulating Light

Metamaterial technology offers unparalleled opportunities for light manipulation. Recent developments in the field of Metamaterial have fuelled new opportunities for engineering space for light propagation, opening a new paradigm in spin and quantum related phenomena in optical physics. Nonlinear Metamaterial is an emerging research topic, whose properties depend on the intensity of EM waves, offer novel phenomena such as hysteretic transition[23], unusual wave mixing[24] and solitary wave propagation[25-26]. The other interesting phenomenon is the reversed Manley–Rowe relation and backward phase matching condition for second-harmonic generation (SHG) or optical parametric amplification (OPA) [27]. Suppose a Metamaterial has a negative refractive index at the fundamental frequency ω_1 and a positive refractive index at the second-harmonic frequency ω_2. At ω_1 the energy flow (Poynting vector) points from left to right, for example; then the wave vector $\overrightarrow{k_1}$ must point from right to left arising from negative index sample at ω_1. The phase matching condition i.e. $\overrightarrow{k_2} = \overrightarrow{2k_1}$ requires that the wave vector $\overrightarrow{k_2}$ at the second harmonic frequency ω_2 also travels from the right to the left. Since the Metamaterial possesses a positive refractive index at ω_2, the energy flow is at the same direction with the wave vector. As a result, the second harmonic signal is maximal at the incident interface rather than the exit interface of the Metamaterial slab, in sharp contrast to SHG in normal dielectric materials as shown in Figure (7). Moreover, artificial magnetic Metamaterial could provide additional routes to boost the nonlinear process[28]. In terms of applications, tunable metamaterials[29-30] and memory devices[31] have been experimentally demonstrated based on nonlinear Metamaterial composites.

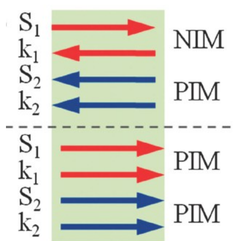

Fig. 7: A typical schematic of SHG (second harmonic generation) when NIMs (negative index materials) are involved, in comparison with normal SHG in only PIMs (positive index materials)

Metamaterial may manifest fascinating phenomenon in the quantum world. In principle, the concept of Metamaterial could be applied to any wave at any scale, including the matter wave which is the wave description of particles, such as electrons and neutrons, in quantum mechanics. Indeed, researchers have taken theoretical efforts towards this direction. Cheianov et al. theoretically demonstrated that negative refraction and focusing of electrons can be achieved in Graphene as shown in Figure (8), a monolayer of graphite[32].

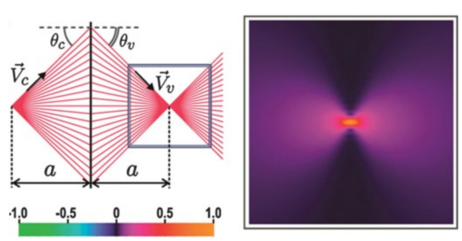

Fig. 8: shows the focusing of electrons by a Graphene p–n junction: (a) the left panel plots the trajectories of electrons, diverging from a source at the distance *a* from the junction and becoming convergent after negative refraction., and the right panel shows the interference-induced pattern in the charge current near the focal image[32]

Figure (9) illustrates the technology and transformation optics approach that enables unprecedented design flexibility and novel device applications.

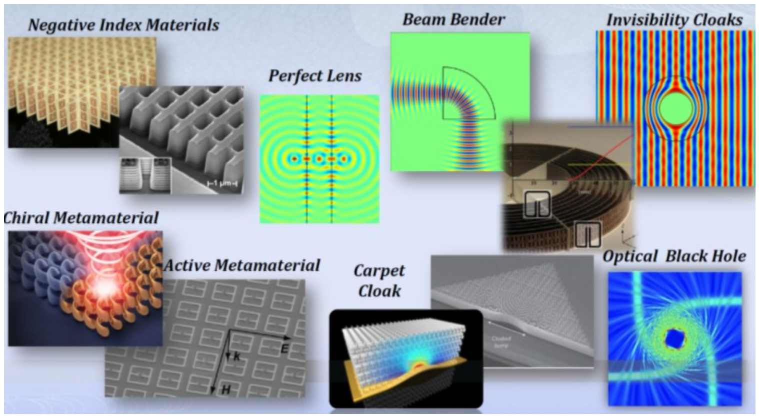

Fig 9. Shows the Metamaterial technology and transformation optics approaches

Metamaterial Technology Challenges

The Metamaterial technology and transformation optics as depicted in Figure (9) facilitate an unparalleled opportunities but at the same time Metamaterial composites fabrication is a challenging tasks. The real challenge is to predict the topology and geometry of negative index microstructures even though they tend to have simple shapes. The topology optimization method allows selection of geometric and topological configuration of multi-physical functional materials while taking into account the MMS material composition. Commercialization of negative index structure is primarily a manufacturing problem because lack of effective tools to economically pattern large volumes of material. Considering the various interesting applications in the field of material science, electronics, optics, and biomedical, it is desirable to improve the Metamaterial fabrication technology. The immediate step envisages improving the homogenization methodology of multi-functions nonlinear Metamaterial devices, improving the bandwidth, and designing smaller. More investigation needed, for example pulse propagation in optical fiber and speed control by means of nonlinear refractive index for the Space-time cloak, Solitons and their variants in negative refractive index composites.

Futuristic Direction

The emerging future is likely to be in the area of Gravitational Casimir effect and signal processing where the space-time cloak acts as a means of prioritizing data channels, rather than theoretically attempt to combine space-time and spatial cloaks. In addition to this, Möbius transformations that exploit hyperbolic characteristics could be interesting for a variety of Minkowski-based relativistic scenarios including spinning cosmic strings.

Gravitational Casimir effect

Figure (10) shows the practical evidence of Casimir force 'F' on parallel plates kept in vacuum, the effective force $F \propto A/d^4$, where *A* is the area of plate and *d* is the distance between the plates. The Casimir force[67] (Figure 11) arises from the interaction of the surfaces with the surrounding electromagnetic spectrum, and includes a complex dependence on the full dielectric function of both surfaces and the region between. On the more theoretical side, MMI structure can produce a powerful Casimir Effect (Force from nothing), which will allow us to transport the matter; this implies that we can use this effect to attract or push away physical matter.

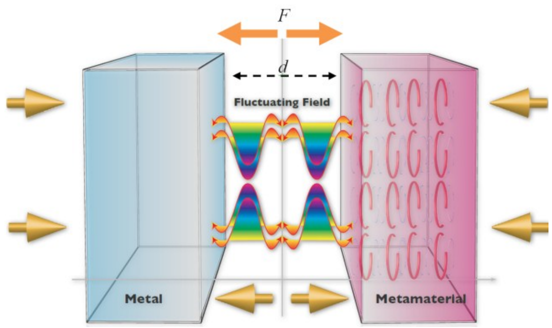

Fig.10: Shows the repulsive Casimir force 'F' on parallel plate kept in vacuum, the effective force F $\propto$- A/d^4, where A is the area of plate and d is the distance between the plate[56].

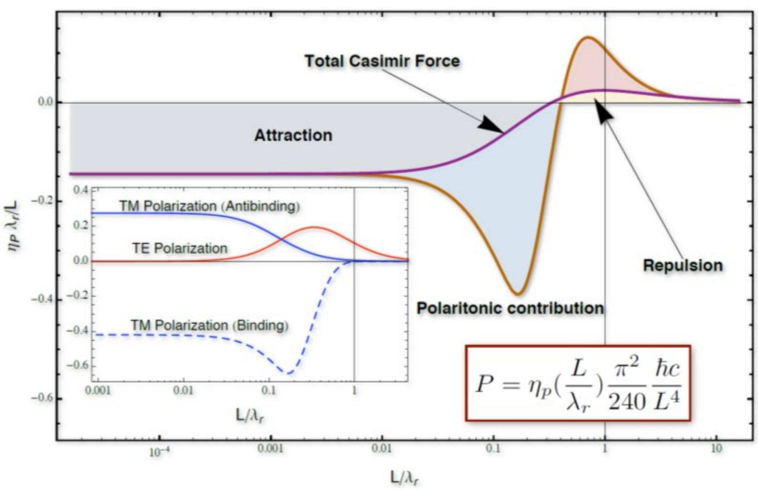

Fig 11. Shows that the polaritonic contribution is responsible for the change in sign of the Casimir force between a metallic and a Metamaterial mirror[56]

As shown in Figure (12)[56], the polaritonic contribution is responsible for the change in sign of the Casimir force between a metallic and a Metamaterial mirror. For $L \geq \lambda_r/5$ the binding TM polariton, which dominates at short distance, is overwhelmed by the joint repulsion due to the anti-binding TM and TE polaritons. This shows that, also for a mixed configuration, surface plasmons are crucial in determining not only the strength and the sign of the Casimir interaction.

One of the exciting properties of MMI structure is that they can bend light in a way that is mathematically equivalent to the way space-time bends light, allows topological exploration for the realization of low cost gravitational wave detector. Figure (12) shows the Gravitational Casimir effect, with a two plate setup, the change in the refractive index of the plates causes the gravitational wave to refract, where *k* represents the wave vector of the incident, transmitted, and reflected gravitational waves, and *γ* is the corresponding angle with respect to the surface normal [68].The Casimir effect has also been investigated in weak gravitational fields to see the effect the slightly curved space time background would have on the Casimir energy [68].

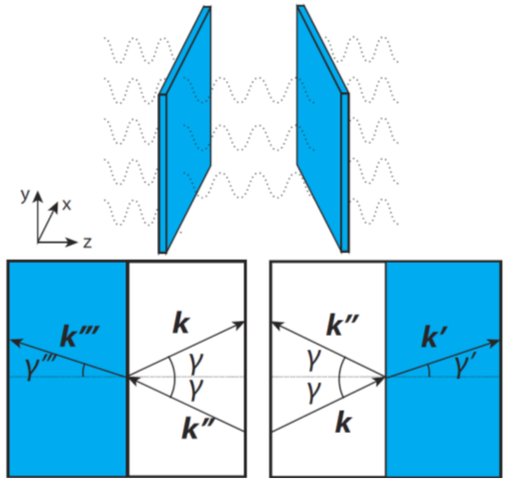

Fig. 12: Shows the Gravitational Casimir effect, with a two plate setup, the change in the refractive index of the plates causes the gravitational wave to refract, where k represents the wave vector of the incident, transmitted, and reflected gravitational waves, and γ is the corresponding angle with respect to the surface normal [68].

Gravitational Wave Reflector

Thin Metamaterial superconducting films are predicted to be highly reflective mirrors for gravitational waves at microwave frequencies. The quantum mechanical non-localizability of the negatively charged Cooper pairs, which are protected from the localizing effect of decoherence by an energy gap, causes the pairs to undergo non-picturable, non-geodesic motion in the presence of a gravitational wave[57]. This non-geodesic motion, which is accelerated motion through space, leads to the existence of mass and charge super currents inside the Metamaterial superconducting film. On the other hand, the decoherence-induced localizability of the positively charged ions in the lattice causes them to undergo picturable, geodesic motion as they are carried along with space in the presence of the same gravitational wave. The resulting separation of charges leads to a virtual plasma excitation within the film that enormously enhances its interaction with the wave, relative to that of a neutral super fluid or any normal matter. The existence of strong mass super currents within a superconducting film in the presence of a gravitational wave, dubbed the H-C (Heisenberg-Coulomb) effect, implies the specular reflection of a gravitational microwave from a film whose thickness is much less than the penetration depth of the material, in close analogy with the electromagnetic case. The argument is developed by allowing classical gravitational fields, which obey Maxwell-like equations, to interact with quantum matter, which is described using the BCS and Ginzburg-Landau theories of superconductivity, as well as a collisionless plasma model.

Experiments at the frontiers of quantum mechanics and gravitation are rare. Minter [57]et al argue for a claim that may lead to several new types of experiment, namely, that a superconducting film whose thickness is less than the London penetration depth of the material can specularly reflect not only electromagnetic (EM) microwaves, as has been experimentally demonstrated [58-59] but gravitational (GR) microwaves as well. The basic motivation lies in the well known fact that Einstein's field equations lead, in the limits of weak GR fields and non-relativistic matter, to gravitational Maxwell-like equations[60], which in turn lead to boundary conditions for gravitational fields at the surfaces of the superconducting films homologous to those of electromagnetism. All radiation fields, whether electromagnetic or gravitational, will be treated classically, whereas the superconductors with which they interact will be treated quantum mechanically.

The first claim is that a GR microwave will generate quantum probability super currents, and thus mass and electrical super currents, inside a superconductor, due to the quantum mechanical non-localizability of the Cooper pairs within the material. The non-localizability of Cooper pairs, which is ultimately due to the Uncertainty Principle (UP), causes them to undergo non-picturable, non-geodesic motion in the presence of a GR wave. This non-geodesic motion, which is accelerated motion through space, leads to the existence of mass and charge super-currents inside a superconductor. By contrast, the localizability of the ions within the superconductor's lattice causes them to undergo picturable, geodesic motion, i.e., free fall, in the presence of the same wave. The resulting relative motion between the Cooper pairs and the ionic lattice causes the electrical polarization of the superconductor in the presence of a GR wave, since its Cooper pairs and ions carry not only mass but oppositely signed charge as well.

Furthermore, the non-localizability of the Cooper pairs is "protected" from the normal process of localization, i.e., from decoherence, by the characteristic energy gap of the Bardeen-Cooper-Schrieffer (BCS) theory of superconductivity. The decoherence of entangled quantum systems such as Cooper pairs (which are in the spin-singlet state) is the fundamental cause of the localizability of all normal matter [61].

Minter [57]et claimed that the mass super-currents induced by a GR wave are much stronger than what one would expect in the case of a neutral super-fluid or any normal matter, due to the electrical polarization of the superconductor caused by the wave. This is what referred to as the "Heisenberg-Coulomb (H-C) effect." The magnitude of the enhancement due to the H-C effect (is given by the ratio of the electrical force to the gravitational force between two electrons,

$$\frac{q^2}{4\pi\varepsilon_0 G m_e^2} = 4.2 \times 10^{42} \tag{9}$$

where q is the electron charge, m_e is the electron mass, ε_0 is the permittivity of free space, and G is Newton's constant. The vastness of equation (9) implies the possibility of an enormous back-action of a superconductor upon an incident GR wave, leading to its reflection.

There are four conventionally accepted fundamental force of nature (i) gravitational, (ii) electromagnetic, (iii) strong nuclear, and (iv) weak nuclear. Each one is understood as the dynamics of a field. The gravitational force is modeled as a continuous classical field. Interestingly, of the four fundamental forces of nature, only gravity and electricity have long range, inverse square laws.

The pure number obtained in (9) by taking the ratio of these two inverse-square laws is therefore just as fundamental as the fine structure constant. Because this number is so large, the gravitational force is typically ignored in treatments of the relevant quantum physics. But for a semi-classical treatment of the interaction of a superconductor with a GR wave must account for both the electrodynamics and the gravito-electrodynamics of the superconductor, since both play an important role in its overall response to a GR wave.

Gravitational characteristic impedance of free space

The Maxwell like representation of the Einstein equations of general relativity can be described the coupling of weak GR fields to slowly moving matter. In the asymptotically flat space-time coordinate system of a distant inertial observer, the four equations in SI units are

$$\nabla \times \bar{E}_G = -\frac{\partial \bar{E}_G}{\partial t} \tag{10}$$

$$\nabla \times \bar{B}_G = \mu_G \left(-j_G + \varepsilon_G \frac{\partial \bar{E}_G}{\partial t} \right) \quad (11)$$

$$\nabla . \bar{E}_G = -\frac{\rho_G}{\varepsilon_G} \quad (12)$$

$$\nabla . \bar{B}_G = 0 \quad (13)$$

where the gravitational analog of the electric permittivity ε_G and magnetic permeability μ_G of free space is given by

$$\mu_G = \frac{4\pi G}{c^2} = 9.3 \times 10^{-27} \quad (14)$$

$$\varepsilon_G = \frac{1}{4\pi G} = 1.2 \times 10^9 \quad (15)$$

The value of ε_G is fixed by demanding that Newton's law of gravitation be recovered from the Gauss like law (13), whereas the value of μ_G is fixed by the linearization procedure from Einstein's field equations. These two constants express the strengths of the coupling between sources (i.e., of masses and mass currents, respectively) and gravitational fields, and are analogous to the two constants ε_0 (the permittivity of free space) and μ_G (the permeability of free space), which express the strengths of coupling between sources (charges and charge currents, respectively) and electromagnetic fields in Maxwell's theory.

In the above set of equations, the field $\bar{E}_G$ is the gravito-electric field, which is to be identified with the local acceleration *g* of a test particle produced by the mass density ρ_G, in the Newtonian limit of general relativity. The field $\bar{B}$ is the gravito-magnetic field produced by the mass current density j_G and by the gravitational analog of the Maxwell displacement current density $\varepsilon_G \left(\frac{\partial \bar{E}_G}{\partial t} \right)$ of the Ampere-like law equation (11). The resulting magnetic-like field $\bar{B}_G$ can be regarded as a generalization of the Lense-Thirring field of general relativity. Because these equations are linear, all fields will obey the superposition principle not only outside the source (i.e., in the vacuum), but also within the matter inside the source, provided the field strengths are sufficiently weak and the matter is sufficiently slowly moving. Note that the fields $\bar{E}_G$ and $\bar{B}_G$in the above Maxwell-like equations will be treated as classical fields, just like the fields $\bar{E}_G$ and $\bar{B}_G$in the classical Maxwell's equations.

As noted earlier, Cooper pairs cannot freely fall along with the ionic lattice in response to an incident GR wave because the UP forbids such pairs from having classical trajectories, i.e., from traveling along geodesics. An incident field $\bar{E}$ will therefore cause the Cooper pairs to undergo non-geodesic motion, in contrast to the geodesic motion of the ions inside the lattice. This entails the existence of mass currents (as well as charge currents) from the perspective of a local, freely falling observer who is located near the surface of the superconducting film anywhere other than at its center of mass. These mass currents will be describable by a gravitational version of Ohm's law

$$J_G(\omega) = \sigma_{S,G}(\omega)\bar{E}_{G-INSIDE}(\omega) \quad (16)$$

where $J_G(\omega)$ is the mass-current density at frequency $\omega, \sigma_{S,G}(\omega) = \sigma_{1S,G}(\omega) + i\sigma_{2S,G}(\omega)$ is the complex mass-current conductivity of the film at the frequency ω in its linear response to the fields of the incident GR wave, and $\bar{E}_{G-INSIDE}(\omega)$ is the driving gravito-electric field inside the film at frequency ω.

The existence of these mass currents can also be inferred from DeWitt's minimal coupling rule for superconductors [62]. The real part of the mass conductivity, $\sigma_{1S,G}(\omega)$, describes the superconductor's dissipative response to the incident gravito-electric field, while the imaginary part, $\sigma_{2S,G}(\omega)$, describes its non-dissipative response to the same field. The basic assumption behind equation (16) is that the mass-current density in any superconductor responds linearly to a weak GR wave at the driving frequency. One should view $\sigma_{S,G}(\omega)$ as a phenomenological quantity, which, like the electrical conductivity σ_S, must be experimentally determined. In any case, the resulting optics for weak GR waves will be linear, just like the linear optics for weak EM waves.

An important physical property follows from the above Maxwell-like equations, namely, the characteristic gravitational impedance of free space Z_G [63-65].

$$Z_G = \sqrt{\frac{\mu_G}{\varepsilon_G}} = \frac{4\pi G}{c} = 2.8 \times 10^{-18} \tag{17}$$

This quantity is a characteristic of the vacuum, i.e., it is a property of space-time itself, and it is independent of any of the properties of matter per se. As with $Z_0 = \sqrt{\frac{\mu_0}{\varepsilon_0}} = 377$ ohms in the EM case, $Z_G = \sqrt{\frac{\mu_G}{\varepsilon_G}} = 2.8 \times 10^{-18}$ will play a central role in all GR radiation coupling problems.

In practice, the impedance of a material object must be much smaller than this extremely small quantity before any significant portion of the incident GR-wave power can be reflected. In other words, conditions must be highly unfavorable for dissipation into heat. Because all classical material objects have extremely high levels of dissipation compared to Z_G, even at very low temperatures, they are inevitably very poor reflectors of GR waves[65-66]. The question of GR-wave reflection from macroscopically coherent quantum systems such as superconductors requires a separate analysis due to the effectively zero resistance associated with superconductors, i.e., the dissipationlessness exhibited by matter in this unique state, at temperatures near absolute zero.

Peters [78] reported the gravitational refractive index n_G, which was much larger than that generated by just considering the induced quadruple moments, suggesting that his model encapsulates the dominant GW interaction with matter, given as

$$n_G = 1 + \frac{2\pi G\rho}{\omega^2} \tag{18}$$

where ρ is the density of the medium.

Minter [57] et al. give the reflection coefficient of a superconducting film from an incident GW as

$$r_G = \frac{1}{1+\frac{2\delta^2}{c\times d}\xi} \tag{19}$$

where δ is the EM skin depth of the superconducting film and d the film thickness.

From (19), the gravitonic contribution to Casimir pressure for superconducting lead (Pb) of thickness d = 2nm at zero temperature is plotted in Figure (14). The EM skin depth of Pb is δ = 37 nm. This is compared with the photonic contribution to the Casimir pressure of superconducting lead. The EM reflection coefficient is [79]

$$r_E = \frac{1}{1+\frac{2\lambda\delta^2}{c\times d}\xi} \tag{20}$$

where λ = 83 nm is the coherence length. The photonic contribution to the Casimir pressure is calculated by using Eq. (19).

James [68] claims that if measurements of the Casimir pressure plots shown in Figure (13) solid line, then one should conclude that the H-C effect is invalid, if we are to hold on to the idea of the graviton. However, if experiments show the Casimir pressure to be
an order of magnitude larger than that predicted from the photonic contribution alone, this would be the first experimental evidence for the validity of the H-C theory and the existence of gravitons. This would open a new field in the way of graviton detection.

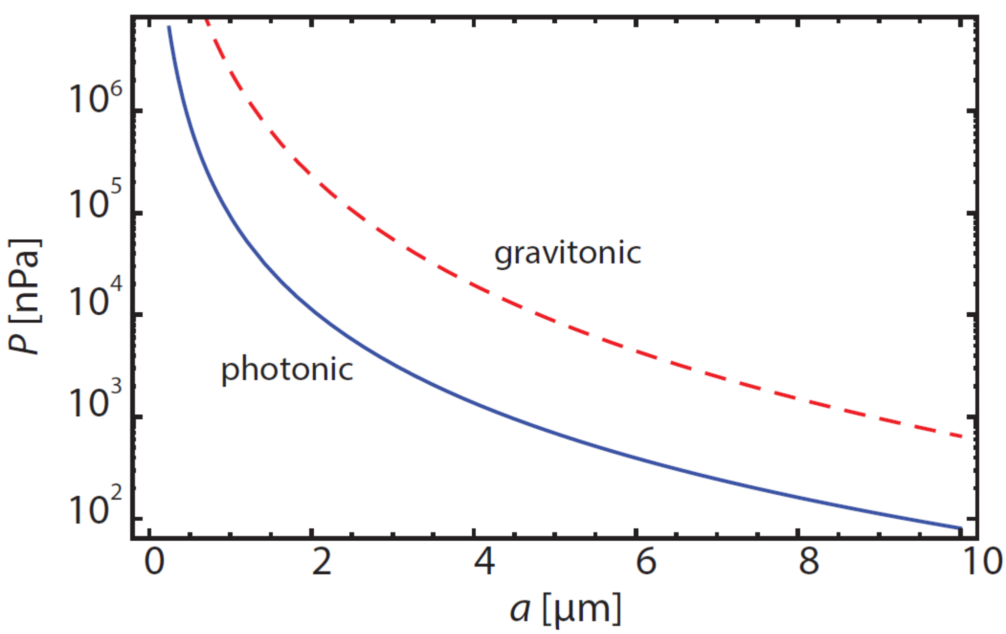

Fig. 13. Gravitonic (dotted line) and photonic (solid line) contributions to the Casimir pressure of parallel plates of superconducting Pb at zero temperature, as a function of plate separation a. Due to the Heisenberg-Coulomb effect,the gravitonic contribution exceeds the photonic [68].

Conclusions

Without any doubt, Metamaterial have become an extremely exciting research area. The unique electromagnetic properties provided by Metamaterial attract considerable attention of researchers from multiple disciplines. In turn, this will spark the merging of knowledge and expertise across different areas, further driving the astounding advance of metamaterial research. Microwave interferometer using metamaterial allows non-invasive detection to liquid chemical-mixture determination[42-43].Within only ten years, we have witnessed many remarkable breakthroughs, such as negative refraction, super lens and invisible cloak. Many other fascinating discoveries and applications are waiting for us to explore. With the complete degree of freedom to control over material properties, what we could do next is only limited by our imagination. Magneto electric couplings can be a source of new behavior in Casimir systems. Metamaterial Casimir repulsive effect leads to anti-gravity and low cost solution for levitation. In this series (Part-1, Part-2, and Part-3), authors have discussed the opportunities and challenges promoted by the scientists, experimentalists and technologists whose focus is in translating negative index composites into practical systems and devices. As a final comment, authors acknowledge that Metasurface made of MMS (Möbius Metamaterial Strips) can provide nearly infinite group delay, very helpful in understanding Einstein Precession, Geodetic Effect and new evidence that requires refining our understanding of the relativistic corrections to Newtonian Celestial Mechanics. For example, multi-knots Möbius strips can be considered as tiny strings that can vibrate in multiple dimensions, and depending on how they vibrate, they might be seen in 3-dimensional space as matter, light or gravity. The vibration of the string which determines whether it appears to be matter or energy, and every form of matter or energy is the result of the vibration of string. Authors consciously set out to provide model of universe as a "Möbius Universe", universe is unbounded without boundary in the form of Möbius loop along the plane of space-time fabrics.

Acknowledgments
Authors would like to thank Dr. Ignaz Eisele (EMFT, Munich, Germany), Dr. Karl-Heinz Hoffmann (Bayerische Akademie, Germany), Dr. Shiban Koul (IIT-Delhi, India), Dr. Tatsuo Itoh (UCLA, USA), and Dr. Rudolph Matthias (BTU Cottbus, Germany) for their valuable inputs, technical discussions, and developing prototype for the experimental validation.

Conclusions

Authors have discussed the opportunities, emerging trends, challenges, and future direction promoted by the scientists, experimentalists and technologists whose focus is in translating Metamaterial into practical systems and devices. The unique electromagnetic properties provided by Metamaterial attract considerable attention of researchers from multiple disciplines. With the complete degree of freedom to control over material properties, what we could do next is only limited by our imagination. Magneto electric couplings can be a source of new behavior in Casimir systems, Metamaterial Casimir repulsive effect can lead to anti-gravity and low cost solution for levitation. As a final comment, authors acknowledge that Metasurface made of MMS (Möbius Metamaterial Strips) can provide nearly infinite group delay, very helpful in understanding Einstein Precession, Geodetic Effect and new evidence that requires refining our understanding of the relativistic corrections to Newtonian Celestial Mechanics. For example, multi-knots Möbius strips can be considered as tiny strings that can vibrate in multiple dimensions, and depending on how they vibrate, they might be seen in 3-dimensional space as matter, light or gravity. The vibration of the string which determines whether it appears to be matter or energy, and every form of matter or energy is the result of the vibration of string. Authors consciously set out to provide model of universe as a "Möbius Universe", universe is unbounded without boundary in the form of Möbius loop along the plane of space-time fabrics.

Acknowledgments
A special heartfelt thank goes to our close friend Late Prof. D. Sundararajan who passed away on 22 September 2014. Prof. Sundararjan and Dr. Poddar had been working on this mysterious Metamaterial

Mobius strips since 1990. Prof. Sundararajan and Dr. Poddar were the first one to demonstrate Mobius strips sensors for the applications in underground mine detections, memory devices and RFID for the detection of chemical explosive and weapons made of plastics and composite materials which were often missed and undetected by RADAR. The Authors would like to thank Dr. Ignaz Eisele (EMFT Fraunhofer Institute, Munich, Germany) for developing prototypes and custom structures, Dr. Karl-Heinz Hoffmann (Bavarian Academy of Science, Germany), Dr. Shiban Koul (IIT-Delhi, India), Dr. Tatsuo Itoh (UCLA, USA), Dr. Matthias Rudolph (BTU Cottbus, Germany), Dr. Afshin Daryoush (Drexel University, Philadelphia, USA), and Dr. Arye Rosen (Rowan University, NJ, USA) for their valuable inputs, technical discussions, and developing prototype for the theoretical proof and experimental validation. The authors also like to thank Indian Government in 1990's for supporting the negative index Möbius strips based RF&MW components for space applications.

Reference

[1] Smith et al, "Determination of effective permittivity and permeability of Metamaterials from reflection and transmission coefficients," *Phys.Rev. B*, Vol. 65, No. 19, 195104, 2002

[2] Smith et al, "Electromagnetic parameter retrieval from inhomogeneous Metamaterials," Phys. Rev. E, Vol. 71, No. 3, 36617, 2005.

[3] Pendry et al, "Low frequency plasmons in thin-wire structures", *J. Phys.: Condens., Matter*, Vol. 10, No. 22, pp. 4785-4809, Jun. 1998.

[4] Pendry et al, Phys. Rev. Lett., 1996, 76, 4773–4776.

[5] Pendry et al, IEEE Trans. Microwave Theory Tech., 1999, 47, 2075–2084.

[6] J. D. Jackson, Classical Electromagnetics, John Wiley & Sons, New York, 3rd edn, 1999.

[7] V. G. Veselago, Sov. Phys. Usp. (Engl. Transl.), 1968, 10, 509–514.

[8] Y. Liua and X. Zhang, "Metamaterials: a new frontier of science and technology", *Chem. Soc. Rev.,* 2011, 40, 2494–2507

[9] Smith et al, Phys. Rev. B: Condens. Matter, 2002, 65, 195104.

[10] Chen et al, Phys. Rev. E: Stat. Phys., Plasmas, Fluids, Relat. Interdiscip. Top., 2005, 71, 046610.

[11] Smith et al, Phys. Rev. E: Stat. Phys., Plasmas, Fluids, Relat. Interdiscip. Top., 2005, 71, 036617.

[12] Menzel et al, Phys. Rev. B: Condens. Matter, 2010, 81, 035320.

[13] Shelby et al, Science, 2001, 292, 77–79.

[14] Xiao et al, Opt. Lett., 2009, 34, 3478–3480.

[15] Zhang et al, Phys. Rev. Lett., 2005, 95, 137404.

[16] Dolling et al, Science, 2006, 312, 892–894.

[17] Wiltshire et al, Science, 2001, 291, 849–851.

[18] Caloz et al, IEEE Trans. Microwave Theory Tech., 2004, 52, 980–992.

[19] Kurs et al, Science, 2007, 317, 83–86.

[20] J. B. Pendry, Phys. Rev. Lett., 2000, 85, 3966–3969.

[21] X. Zhang and Z. W. Liu, Nat. Mater., 2008, 7, 435–441.

[22] N. Fang, H. Lee, C. Sun and X. Zhang, Science, 2005, 308, 534–537.

[23] Zharov et al, Phys. Rev. Lett., 2003, 91, 037401.

[24] Agranovich et al, Phys. Rev. B: Condens. Matter, 2004, 69, 165112

[25] Lazarides et al, Phys. Rev. Lett., 2006, 97, 157406

[26] Liu et al, Phys. Rev. Lett., 2007, 99, 153901

[27] Litchinister and V. M. Shalaev, Laser Phys. Lett., 2008, 5, 411–420.

[28] Klein et al, , Science, 2006, 313, 502–504.

[29] Shadrivov et al, , Opt. Express, 2006, 14, 9344–9349.

[30] Wang et al, Opt. Express, 2008, 16, 16058–16063.

[31] Driscoll et al, Science, 2009, 325, 1518–1521

[32] Cheianov et al, Science, 2007, 315, 1252–1255.

[33] Zhang et al, Phys. Rev. Lett., 2008, 100, 123002.

[34] Jacob et al, Appl. Phys. B: Lasers Opt., 2010, 100, 215–218.

[35] Noginov et al, Opt. Lett., 2010, 35, 1863–1865.

[36] C. Henkel and K. Joulain, Europhys. Lett., 2005, 72, 929–935.

[37] U. Leonhardt and T. G. Philbin, New J. Phys., 2007, 9, 254.

[38] Rosa et al, Phys. Rev. Lett., 2008, 100, 183602.

[39] Zhao et al, Phys. Rev. Lett., 2009, 103, 103602.

[40] V. Yannopapas and N. V. Vitanov, Phys. Rev. Lett., 2009, 103, 120401.

[41] S. I. Maslovski and M. G. Silveirinha, Phys. Rev. A, 2010, 82, 022511.

[42] Yang et al, "Distinguishing the viability of a single yeast cell with an ultra-sensitive radio frequency sensor," Lab Chip, vol. 10, pp. 553–555, 2010.

[43] Y. Cui and P. Wang, "The design and operation of ultra-sensitive and tunable radio-frequency interferometers," IEEE TMTT, vol. 62, no. 12, pp. 3172–3182, Dec 2014.

[44] Agrawal G. P. Fiber-Optic Communication Systems, 3rd ed, Wiley 2010.

[45] Gnauck et al, "High-capacity optical transmission systems", J. Light wave Technol. 26, 1032–1045 (2008).

[46] Essiambre R. J. & Tkach R. W. Capacity trends and limits of optical communication networks. Proc. IEEE 100, 1035–1055 (2012).

[47] Gnauck A. H. *et al.* Spectrally efficient long-haul WDM transmission using 224-Gb/s polarization-multiplexed 16-QAM. J. Light wave Technol. 29, 373–377 (2011).

[48] Richardson et al , Space-division multiplexing in optical fibres. Nature Photonics 7, 354–362 (2013).

[49] Fini J. M. *et al.* High-Capacity Space-Division-Multiplexed DWDM Transmissions Using Multi core Fiber. J. Light wave Technol. 30, 486–492 (2012).

[50] Liu X. *et al.* 1.12-Tb/s 32-QAM-OFDM, Opt. Express 19, B958–B964 (2011).

[51] Ryf R. *et al.* Mode-division multiplexing over 96 km of few-mode fiber using coherent 6 × 6 MIMO processing. J. Lightwave Technol. 30, 521–531 (2012).

[52] Bozinovic N. *et al.* Terabit-Scale Orbital Angular Momentum Mode Division Multiplexing in Fibers. Science 340, 1545–1548 (2013)

[53] Bozinovic N., Golowich S., Kristensen P. & Ramachandran S. Control of orbital angular momentum of light, with optical fibers. Opt. Lett. 37, 2451–2453 (2012)

[54] Gregg P. *et al.* Stable Transmission of 12 OAM States in Air-Core Fiber, in CLEO: 2013, OSA Technical Digest. (Online) (Optical Society of America, 2013), paper CTu2K.2.

[55] J. Zeng, et al. "Manipulating Complex Light with Metamaterial", Scientific reports, Sept 2013

[56] http://cnls.lanl.gov/casimir/PostersSF/Intravaia-SantaFe-poster.pdf

[57] S. Minter, K. Wegter-McNelly, and R. Chiao," Do mirrors for gravitational wave exist?", http://arxiv.org/abs/0903.0661v10

[58] R.E. Glover, M. Tinkham, Phys. Rev. 104 (1956) 844.

[59] M. Tinkham, Introduction to Superconductivity, 2nd ed., Dover, New York, 2004.

[60] Braginsky et al, General relativity, University of Chicago, Chicago, 1984

[61] W.H. Zurek, Rev. Mod. Phys. 75 (2003) 715; H. Ollivier, D. Poulin, W.H. Zurek, Phys. Rev. Lett. 93(2004) 220401.

[62] B.S. DeWitt, Phys. Rev. Lett. 16 (1966) 1092.

[63] Chiao et al in Science and Ultimate Reality, arXiv:quant-ph/0303100.

[64] C. Kiefer, C. Weber, Ann. der Phys. (Leipzig) 14 (2005), 253.

[65] Chiao et al, Proceedings of the Time & Matter Conference, Venice, Italy, 11-17 August 2002, I. Bigi and M. Faessler (Eds.), World Scientific, Singapore, 2006; arXiv:gr-qc/0303089.

[66] S. Weinberg, Gravitation and Cosmology, Wiley, New York, 1972.

[67] Astrid Lambrecht, "The Casimir effect: a force from nothing", Physics World, Sept 2002, IOP Publishing Ltd 2014, ISSN: 0953-8585

[68] James Q. Quach, "Gravitational Casimir effect", Phys. Rev. Lett. 114, 081104 (2015)

[69] Ulrich L. Rode, Ajay K. Poddar, " Möbius Metamaterial inspired next generation circuits and systems", Microwave Journal, May 2016

[70] Ulrich L. Rode, Ajay K. Poddar, "Möbius Metamaterial Inspired: Signal Sources and Sensors ", Microwave Journal, June 2016

[71 Ulrich L. Rohde, Ajay K. Poddar, "Ka-Band Metamaterial Möbius Oscillator (MMO) Circuit", IEEE IMS MTT-S Digest, pp. 1-4, 2016

[72] U. L. Rohde, A. K. Poddar, "Möbius Metamaterial Strips Resonator: Tunable Oscillators for Modern Communication Systems", Microwave Journal, Jan 2015

[73] U. L. Rohde, A. K. Poddar, "Metamaterial Resonators: Theory and Applications", Microwave journal, Dec 2014, pp. 74-86.

[74]U. L. Rohde, A. K. Poddar, "Möbius Strips and Metamaterial Symmetry: Theory and Applications", Microwave journal, Nov 2014, pp. 76-88.

[75] U. L. Rohde, A. K. Poddar, D. Sundararjan "Printed Resonators: Möbius Strips Theory and Applications" ", Microwave journal, pp. 24-54, Nov 2013.

[76] C. Scarborough, et al., Appl. Phys. Le(.,101,014101(2012).

[77] Jiang et al, *IEEE Antennas and Wireless Propagation Letters,* vol. 10, pp. 1543-1546 (2011).

[78] P. C. Peters, Phys. Rev. D 9, 2207 (1974)

[79] Minter et al, Physica E 42, 234 (2010).